Journal of Fundamental and Applied Research **Vol. 5**, Issue 2 (2025) **20250007**

Received: 06 May 2025 / Accepted: 25 June 2025
Published online: 27 June 2025
© 2025 The Author(s)

Geometrical structure and stable circular orbits near regular black holes in Verlinde's emergent gravity

Mardon Abdullaev,[1,2,*] Nurmuxammed Aytimbetov,[3,†] and Gumisbek Allambergenov[4,‡]

[1] *Institute of Fundamental and Applied Research, National Research University TIIAME, Kori Niyoziy 39, Tashkent 100000, Uzbekistan*
[2] *Institute of Nuclear Physics, Ulugbek 1, Tashkent 100214, Uzbekistan*
[3] *Namangan State University, Boburshok 161, 160107, Uzbekistan*
[4] *Karakalpak State University, Nukus 230100, Uzbekistan*

Abstract. We investigate the geometrical structure and orbital dynamics of regular black holes in the framework of Verlinde's emergent gravity. By constructing a modified spherically symmetric spacetime that incorporates both baryonic and entropy-induced gravitational effects, we analyze the behavior of the metric function and explore the conditions for the existence of stable circular orbits. We derive the radii of characteristic orbits such as the innermost stable circular orbit (ISCO), marginally bound orbit (MBO), and photon sphere, and examine how these are influenced by the emergent gravity parameter and regularization scale. Furthermore, we compute the Keplerian, radial, and vertical epicyclic frequencies of test particles and apply the relativistic precession (RP) model to predict twin-peak quasiperiodic oscillations (QPOs). Our findings show that entropy-based corrections significantly affect spacetime geometry and observable frequencies, suggesting that high-frequency QPOs may offer a viable tool for probing Verlinde-type gravity in strong-field regimes.

Keywords: Quasiperiodic oscillations, emergant gravity, dark matter, regular black hole.

I. INTRODUCTION

The study of black holes has evolved from a mathematical curiosity to a cornerstone of modern astrophysics. Observational evidence, including the direct imaging of black hole shadows by the Event Horizon Telescope (EHT) and gravitational wave detections by LIGO and Virgo, has confirmed the presence of compact objects consistent with black holes at the centers of galaxies and in binary systems. These observations provide a unique opportunity to test gravitational theories in the strong-field regime [1].

One of the intriguing recent developments in theoretical physics is the emergent gravity scenario proposed by Verlinde [2]. According to this framework, gravity is not a fundamental interaction but an emergent phenomenon arising from changes in the information associated with the positions of material bodies. Notably, Verlinde's theory introduces an additional gravitational component — the so-called "apparent dark matter" — which results from the entropy variation due to the presence of baryonic matter in a universe with positive cosmological constant.

This modified description of gravity has profound implications for spacetime geometry and the nature of compact objects such as black holes. In particular, it allows for the construction of regular black hole solutions in which the central singularity is removed due to quantum or geometric effects. These regular black holes, when embedded in Verlinde's emergent gravity framework, exhibit new phenomenology in their spacetime structure [3, 4].

The primary objective of this work is to investigate the geometrical structure and the behavior of stable circular orbits around regular black holes that emerge in Verlinde's gravity. By analyzing the effective potential for test particle motion, we identify conditions for the existence of innermost stable circular orbits (ISCOs), marginally bound orbits (MBOs), and photon spheres. Additionally, we explore the implications of these orbits for astrophysical observables such as quasiperiodic oscillations (QPOs), which serve as potential probes of the underlying spacetime geometry [5, 6].

* Corresponding author: mardonabdullaev@gmail.com
† nurmuxammedzaytimbetov@gmail.com
‡ gumisbekallambergenov@gmail.com

This paper is organized as follows: In Section III, we review the construction of regular black hole solutions within Verlinde's emergent gravity. Section IV focuses on the motion of test particles and the derivation of effective potentials. In Section V, we compute the fundamental frequencies of circular motion and relate them to observational phenomena. Finally, in Section VI, we discuss the possible observational signatures in the context of QPO models and present our conclusions in Section VII.

II. OVERVIEW OF EMERGENT GRAVITY AND MOTIVATIONS

Black holes are among the most fascinating and fundamental objects in theoretical physics and observational astronomy. Traditionally, they have served as critical testbeds for general relativity (GR), especially in the strong-field regime. Recent advances in astrophysical observations, such as the imaging of the supermassive black hole shadow by the Event Horizon Telescope (EHT) [7] and the detection of gravitational waves by LIGO/Virgo [8], have provided direct evidence for the existence of black holes, confirming their physical reality and not just their mathematical origin.

Despite the success of general relativity, it fails to fully explain the observed flat rotation curves of galaxies, the dynamics of galaxy clusters, and the accelerated expansion of the universe without invoking hypothetical components such as dark matter and dark energy. One alternative perspective to address these challenges is provided by Verlinde's emergent gravity theory [2]. This approach views gravity not as a fundamental interaction, but as an emergent, entropic force resulting from the microscopic degrees of freedom associated with spacetime.

Verlinde postulates that the presence of baryonic matter reduces the entropy of the universe by affecting the microscopic configurations of spacetime. This reduction induces an elastic response in the underlying medium, which manifests as an additional gravitational attraction. Remarkably, this extra force reproduces many of the phenomena attributed to dark matter without introducing new particles. In particular, emergent gravity offers a natural explanation for the flattening of galactic rotation curves and the Tully-Fisher relation [9, 10].

In this context, it becomes essential to explore how black hole geometries are modified in emergent gravity. By constructing regular black hole solutions that avoid singularities and incorporate entropy-based corrections [3, 4], one can investigate the resulting spacetime structure and its influence on test particle dynamics. The study of circular orbits, effective potentials, and fundamental frequencies around such black holes enables direct comparisons with astrophysical data — especially quasiperiodic oscillations (QPOs), which are sensitive to the local geometry of compact objects [5, 6].

The aim of this paper is to analyze the geometrical structure and stable circular orbits near regular black holes that arise in Verlinde's emergent gravity. By deriving the modified metric, exploring the motion of test particles, and computing orbital frequencies, we seek to identify observational signatures that distinguish emergent gravity black holes from those predicted by classical general relativity.

III. SPACETIME GEOMETRY OF REGULAR BLACK HOLES IN VERLINDE GRAVITY

In the framework of Verlinde's emergent gravity, the gravitational field is modified due to entropy-based corrections related to baryonic matter distribution [2, 9, 10]. This leads to the emergence of an effective "apparent dark matter" component that alters the standard mass profile of spacetime [11]. Following Verlinde's proposal, the apparent dark mass $M_D(r)$ is related to the baryonic mass $M_B(r)$ through the integral relation:

$$\int_0^r \frac{M_D^2(r')}{r'^2}\, dr' = \frac{a_0 M_B(r) r}{6}, \tag{1}$$

where $a_0 = cH_0$ is the characteristic acceleration scale, and H_0 is the Hubble parameter.

Differentiating Eq. (1), we obtain a local expression for $M_D(r)$:

$$M_D^2(r) = \frac{a_0 r^2}{6}\, \frac{d}{dr}\left[r M_B(r)\right]. \tag{2}$$

The total gravitational mass function becomes:

$$m(r) = 4\pi \int_0^r \left[\rho_B(r') + \rho_D(r')\right] r'^2\, dr', \tag{3}$$

and the corresponding spacetime metric is expressed in standard Schwarzschild-like coordinates as:

$$ds^2 = -f(r)dt^2 + \frac{1}{f(r)}dr^2 + r^2\left(d\theta^2 + \sin^2\theta d\phi^2\right), \tag{4}$$

where $f(r)$ is the lapse function encoding the gravitational potential.

To incorporate regularity (i.e., the absence of singularities), we adopt the mass profile proposed by Frolov [3], defined as:

$$M_B(r) = \frac{(Mr - \frac{Q^2}{2})r^3}{r^4 + (2Mr + Q^2)l_0^2}, \tag{5}$$

where Q is the electric charge and l_0 is a parameter controlling the regularization scale. This choice ensures finiteness of curvature scalars at the origin and extends earlier models such as Bardeen [12] and Hayward [4] black holes.

The resulting metric function becomes:

$$f(r) = 1 - \frac{(2Mr - Q^2)r^2}{r^4 + (2Mr + Q^2)l_0^2} - \frac{2\sqrt{a_M K(r)}}{r^4 + (2Mr + Q^2)l_0^2}, \tag{6}$$

with $a_M = a_0/6$ and

$$K(r) = r^3\left[Mr^5 + l_0^2\left(8M^2r^2 + 2MQ^2r - 2Q^4\right)\right]. \tag{7}$$

A. Analysis of the metric function $f(r)$

The function $f(r)$ determines the causal structure of the spacetime. Its zeros correspond to horizons, and its behavior near $r = 0$ reveals regularity.

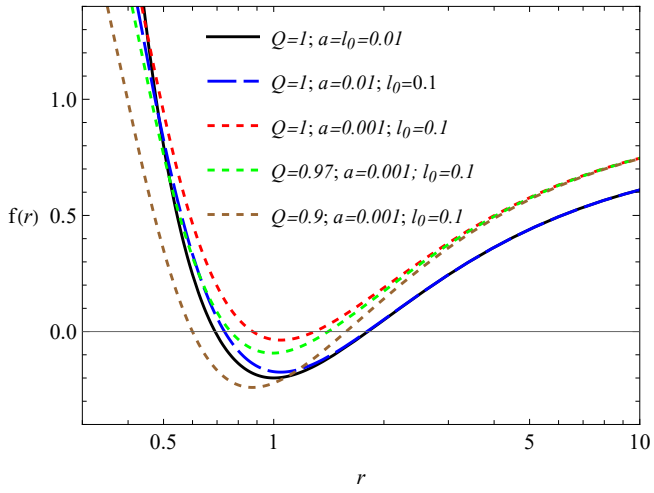


Figure 1. Metric function $f(r)$ for various values of a, Q, and l_0, with fixed $M = 1$. The curves show different horizon structures depending on the parameters.

a. Revised physical interpretation of Fig. 1: Figure 1 illustrates the behavior of the metric function $f(r)$ for various combinations of electric charge Q, regularization scale l_0, and emergent gravity parameter a. The qualitative features reflect how Verlinde-type modifications affect the spacetime geometry:

- The zeros of $f(r)$ identify the locations of the event and Cauchy horizons. Depending on the parameters, one can observe two real positive roots (non-extremal case), a single degenerate root (extremal case), or no horizon (naked core). - At small r, increasing l_0 smoothens the inner structure, suppressing the divergence of curvature invariants and confirming the regular nature of the black hole. - The parameter a, which controls the strength of entropy-induced gravitational corrections, shifts the entire profile of $f(r)$ downward, effectively deepening the gravitational well and modifying the location of horizons. - For increasing Q, the outer horizon radius decreases, consistent with standard charged black hole behavior, but in the presence of $a > 0$, the critical charge for extremality increases — showing a stabilizing effect from emergent gravity.

In summary, the updated figure confirms that entropy-based corrections can significantly alter both the causal structure and near-horizon geometry, offering potential observational signatures distinguishable from standard general relativity.

B. Horizon radius vs. charge dependence

To understand how black hole charge affects the location of the horizon, we plot the outer horizon radius r_h as a function of Q for several values of a and l_0.

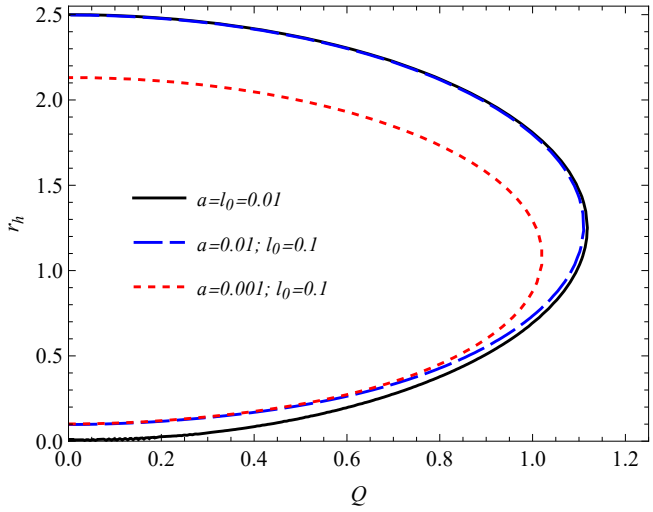


Figure 2. Outer horizon radius r_h versus black hole charge Q for different values of a and l_0. The critical behavior and extremality conditions can be inferred.

a. Physical interpretation of Fig. 2: In Fig. 2, we observe: - For $a = 0$, the dependence of r_h on Q resembles the standard Reissner-Nordström case, with the outer horizon shrinking as Q increases. - For $a > 0$, the curve becomes more nonlinear: the increase in charge does not lead to immediate extremality, indicating a modification in the causal structure due to emergent gravity. - Larger l_0 values generally increase r_h, showing that nonlocal entropy effects effectively "inflate" the horizon radius [11].

Overall, these results indicate that Verlinde-inspired corrections not only regularize the singularity but also modify the near-horizon structure in a way that could affect observational features such as shadow size and QPO frequencies.

IV. CIRCULAR MOTION AND EFFECTIVE POTENTIAL OF TEST PARTICLES

We now examine the motion of neutral test particles in the spacetime geometry constructed in Section III. The dynamics are governed by the Lagrangian

$$\mathcal{L} = \frac{1}{2} m g_{\mu\nu} \dot{x}^\mu \dot{x}^\nu, \tag{8}$$

where m is the particle mass and $g_{\mu\nu}$ is the spacetime metric. Due to the spherical symmetry and static nature of the background, the energy E and angular momentum L per unit mass are conserved [13, 14]:

$$E = -g_{tt}\dot{t}, \qquad L = g_{\phi\phi}\dot{\phi}. \tag{9}$$

Assuming motion confined to the equatorial plane ($\theta = \pi/2$), the normalization condition for timelike geodesics becomes:

$$g_{\mu\nu}\dot{x}^\mu \dot{x}^\nu = -1. \tag{10}$$

This yields the radial equation of motion in the form:

$$\dot{r}^2 + V_{\text{eff}}(r) = E^2, \tag{11}$$

where the effective potential is given by:

$$V_{\text{eff}}(r) = f(r)\left(1 + \frac{L^2}{r^2}\right). \tag{12}$$

A. Circular orbit conditions

Circular orbits correspond to radial turning points where $\dot{r} = 0$ and $\ddot{r} = 0$, leading to:

$$V_{\text{eff}}(r) = E^2, \qquad \frac{dV_{\text{eff}}}{dr} = 0. \tag{13}$$

Solving these equations gives the specific angular momentum and energy of the particle:

$$L^2 = \frac{r^3 f'(r)}{2f(r) - rf'(r)}, \tag{14}$$

$$E^2 = \frac{2f(r)^2}{2f(r) - rf'(r)}. \tag{15}$$

Such expressions are essential for studying stable and unstable orbits in both classical and modified gravity contexts [15].

B. Stability of circular orbits

The stability of circular orbits is determined by the second derivative of the effective potential. The innermost stable circular orbit (ISCO) satisfies:

$$\frac{d^2 V_{\text{eff}}}{dr^2} = 0. \tag{16}$$

Expressed in terms of $f(r)$, the ISCO condition becomes [5]:

$$f'(r)\left(\frac{2rf'(r)}{f(r)} - 3\right) - rf''(r) \geq 0. \tag{17}$$

Other important orbital radii include: - The **photon sphere** (phs), where massless particles can orbit; - The **marginally bound orbit** (MBO), where the total energy equals rest mass ($E = 1$).

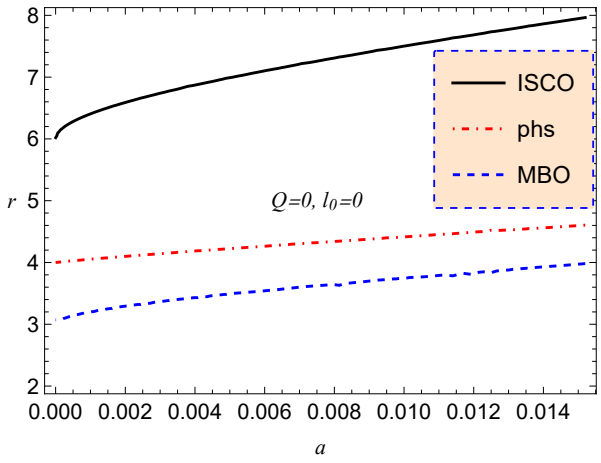


Figure 3. Radial location of characteristic orbits (ISCO, MBO, photon sphere) as functions of emergent gravity parameter a. For $Q = 0$, $l_0 = 0.1$, the curves show the shift of orbital structure.

a. Physical interpretation of Fig. 3: Figure 3 illustrates how the positions of characteristic orbits depend on the emergent gravity parameter a, which represents the entropy-based modification to spacetime. As a increases: - The **photon sphere** moves outward, indicating that null geodesics require larger radii to remain bound, which affects the shadow size of the black hole. - The **marginally bound orbit (MBO)** also shifts to larger radii, suggesting changes in the energy conditions required for bounded particle motion. - The **ISCO** radius increases significantly, implying that stable circular motion for accreting matter becomes possible only at greater distances from the black hole.

These trends reflect the impact of Verlinde's emergent gravity on the effective potential: entropy-induced effects smooth the spacetime geometry, reduce central mass concentration, and reshape the gravitational well. Consequently, the orbital structure is more extended compared to classical GR predictions, which has observable implications in accretion disk physics and QPO modeling.

C. Parametric structure of orbital radii

We also explore how the horizon and orbital radii vary as functions of charge-to-mass ratio Q/M, identifying characteristic resonance zones for twin-peak QPOs [1].

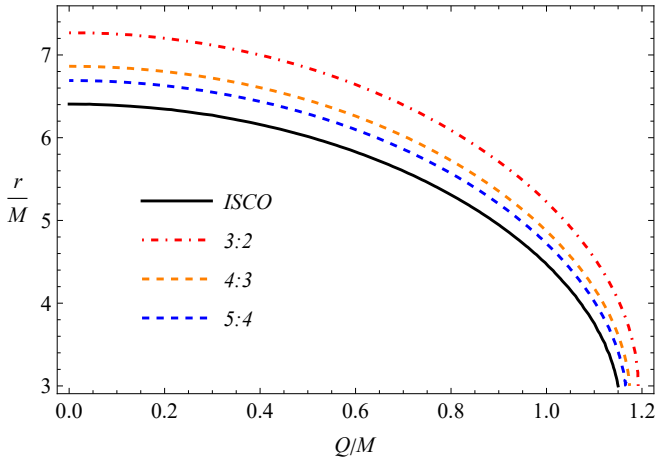


Figure 4. Variation of orbital radii with respect to charge-to-mass ratio Q/M for fixed parameters $l_0 = 0.1$, $a_M = 0.01$. Specific resonant ratios (3:2, 4:3, 5:4) are indicated.

a. Physical interpretation of Fig. 4: Figure 4 shows the variation of orbital radii as a function of Q/M, with emphasis on the locations where epicyclic frequency ratios form simple rational numbers. These resonance points (3:2, 4:3, 5:4) are believed to correspond to observed QPO frequencies in black hole X-ray binaries. - As Q/M increases, the characteristic orbits shift outward, which modifies the frequency structure of circular and radial oscillations. - The presence of resonant points suggests that the emergent gravity spacetime supports conditions favorable for QPO generation.

This plot demonstrates how tuning the black hole charge can shift the resonance zone and influence the orbital motion dynamics of matter in accretion flows. Matching such theoretical predictions to observational QPO data offers a way to constrain the parameter space of Verlinde-type gravity models.

V. ORBITAL, RADIAL, AND VERTICAL FREQUENCIES OF OSCILLATION

The motion of test particles in stable circular orbits around black holes is not perfectly uniform: small perturbations in the radial and vertical directions result in oscillatory motion. These oscillations are characterized by three fundamental frequencies [1, 5, 16]:

- Ω_K — Keplerian (orbital) frequency,
- Ω_r — radial epicyclic frequency,
- Ω_θ — vertical epicyclic frequency.

These frequencies play a central role in interpreting high-frequency QPOs observed in X-ray binaries and can serve as a diagnostic of the underlying spacetime geometry [17, 18].

A. Keplerian frequency

The Keplerian angular frequency Ω_K is defined as the rate of change of azimuthal angle ϕ with respect to coordinate time t [17]:

$$\Omega_K = \frac{d\phi}{dt} = \sqrt{\frac{f'(r)}{2r}}. \tag{18}$$

To express this frequency in physical units (Hz), we use:

$$\nu_K = \frac{1}{2\pi}\frac{c^3}{GM}\,\Omega_K, \tag{19}$$

where c is the speed of light and G is the gravitational constant.

B. Radial and vertical oscillations

Small deviations from the circular orbit in radial ($r \to r_0 + \delta r$) and vertical ($\theta \to \pi/2 + \delta\theta$) directions lead to harmonic oscillations governed by [15]:

$$\frac{d^2\delta r}{dt^2} + \Omega_r^2\,\delta r = 0, \tag{20}$$

$$\frac{d^2\delta\theta}{dt^2} + \Omega_\theta^2\,\delta\theta = 0. \tag{21}$$

The frequencies are given by [5, 18]:

$$\Omega_r^2 = -\frac{1}{2g_{rr}(u^t)^2}\,\frac{\partial^2 V_{\text{eff}}(r,\theta)}{\partial r^2}\bigg|_{\theta=\pi/2}, \tag{22}$$

$$\Omega_\theta^2 = -\frac{1}{2g_{\theta\theta}(u^t)^2}\,\frac{\partial^2 V_{\text{eff}}(r,\theta)}{\partial \theta^2}\bigg|_{\theta=\pi/2}. \tag{23}$$

In terms of the metric function $f(r)$, the explicit expressions for the radial and vertical frequencies become [5]:

$$\Omega_r = \Omega_K \sqrt{\left(3 + \frac{rf''(r)}{f'(r)}\right)\left(f(r) - \frac{1}{2}rf'(r)\right)}, \tag{24}$$

$$\Omega_\theta = \Omega_K. \tag{25}$$

C. Numerical analysis of frequency profiles

We now compute the variation of the Keplerian frequency Ω_K as a function of radial distance r for different values of the regularization parameter l_0 at fixed spin $a = 0.5$.

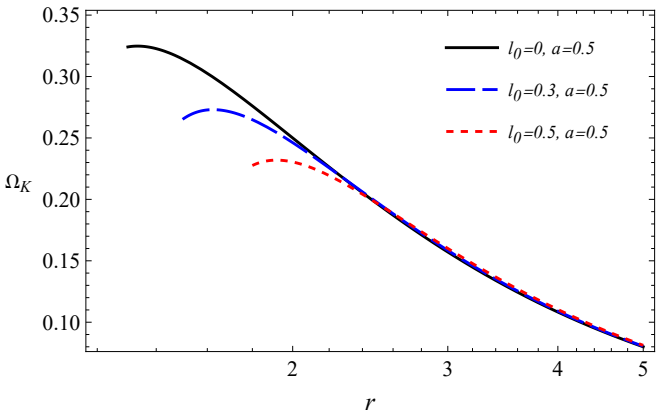


Figure 5. Radial dependence of the Keplerian frequency Ω_K for $a = 0.5$ and varying l_0. The curves show that Ω_K is sensitive to the regularization scale of the black hole geometry.

a. Physical interpretation of Fig. 5: Figure 5 demonstrates how the Keplerian frequency Ω_K changes with radial distance for different values of l_0. The trends reveal the following: - For small r, Ω_K increases as we approach the black hole, then peaks and decreases. - Larger values of l_0 lead to a lower peak value of Ω_K, reflecting a more extended gravitational potential. - The shape of $\Omega_K(r)$ influences the location and strength of QPOs, which are tied to orbital motion.

These results provide a direct connection between the microscopic entropy-based corrections of Verlinde gravity and macroscopic observable signatures [2, 13].

VI. MODELING QUASIPERIODIC OSCILLATIONS AND OBSERVATIONAL IMPLICATIONS

Quasiperiodic oscillations (QPOs) are observed as narrow peaks in the X-ray power spectra of compact objects such as black holes, neutron stars, and white dwarfs. High-frequency QPOs (HFQPOs), in particular, are believed to be closely related to the dynamics of matter in strong gravity near compact objects, typically occurring at orbital frequencies of inner accretion flows [1, 16].

Among various models, the relativistic precession (RP) model [5, 6] provides a physically motivated explanation for twin-peak HFQPOs, where the observed upper and lower frequencies are associated with fundamental motion:

$$\nu_U = \nu_\phi, \tag{26}$$

$$\nu_L = \nu_\phi - \nu_r, \tag{27}$$

where $\nu_\phi = \Omega_K/(2\pi)$ is the azimuthal (Keplerian) frequency and $\nu_r = \Omega_r/(2\pi)$ is the radial epicyclic frequency. These frequencies depend sensitively on the underlying spacetime geometry and can thus serve as observational probes of modified gravity models such as Verlinde's emergent gravity [13, 18].

A. Effective modeling via modified metric

In this section, we analyze the effective gravitational potential and frequency structure predicted by our Verlinde-inspired regular black hole metric, focusing on the variation of frequency bands with parameters such as Q and l_0. We particularly explore how the presence of entropy-based corrections affects the effective potential felt by orbiting matter and the resulting precession frequencies [2].

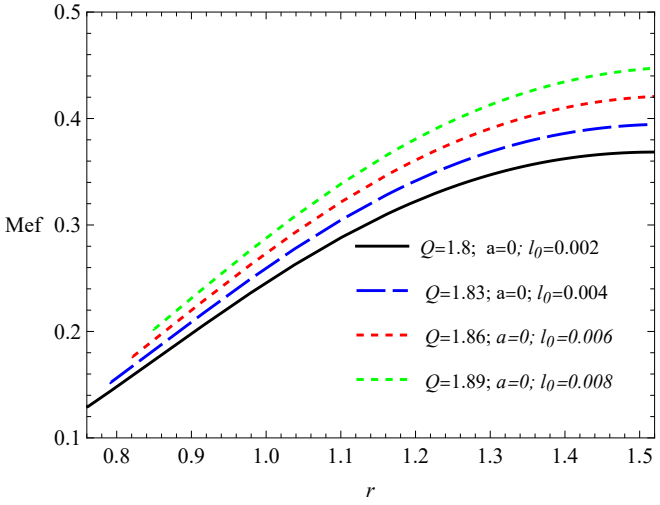


Figure 6. Effective mass function $M_{\text{eff}}(r)$ for various values of Q and l_0, illustrating how the potential well structure is deformed in Verlinde gravity.

a. Physical interpretation of Fig. 6: Figure 6 displays the radial profile of the effective mass function $M_{\text{eff}}(r)$ for several values of electric charge Q and regularization parameter l_0, with fixed $a = 0$. Key insights include: - Increasing Q deepens the effective potential well, leading to higher Keplerian frequencies at small radii [15]. - Larger l_0 values reduce the central mass concentration, flattening the potential profile and thereby lowering ν_ϕ and ν_r. - These modifications shift the ν_U and ν_L curves predicted by the RP model and allow for more precise modeling of observed QPO frequency ratios [17].

Such insights are crucial for distinguishing between regular black holes in emergent gravity and classical Reissner-Nordström or Kerr geometries. Future X-ray timing missions may be able to test these deviations through high-precision measurements of QPOs [16].

VII. SUMMARY AND OUTLOOK

In this paper, we have studied the geometrical structure and orbital properties of regular black holes inspired by Verlinde's emergent gravity. This framework offers a thermodynamic interpretation of gravity where the effects commonly attributed to

dark matter arise naturally from entropy gradients caused by baryonic matter distributions.

We constructed a class of static, spherically symmetric regular black hole solutions using a modified mass profile that incorporates both baryonic and emergent gravity contributions. The resulting metric function $f(r)$ was shown to be regular everywhere and capable of supporting a variety of causal structures depending on the parameters Q, a, and l_0.

Through the analysis of test particle motion, we derived the effective potential and investigated conditions for the existence and stability of circular orbits. We calculated the radii of marginally bound orbits (MBO), photon spheres (phs), and innermost stable circular orbits (ISCO), revealing their sensitivity to the emergent gravity parameter a and the regularization scale l_0.

We further computed the fundamental frequencies — the Keplerian, radial, and vertical oscillation frequencies — which play a key role in modeling high-frequency QPOs. Using the relativistic precession model, we demonstrated how entropy-induced corrections deform the effective gravitational potential, shifting the observable twin-peak QPO frequencies. These findings suggest that QPO measurements can serve as powerful probes of underlying spacetime structure, potentially distinguishing Verlinde-type black holes from classical GR solutions.

Outlook. Future work can extend this analysis by including:

- Rotating (axially symmetric) extensions of regular black holes in Verlinde gravity;
- Comparison with observed QPO data from X-ray binaries such as GRO J1655–40 or XTE J1550–564;
- Investigation of gravitational wave signals from inspiraling particles affected by emergent dark gravity;
- Stability analysis of the spacetime under perturbations.

Such investigations will provide deeper insight into the role of thermodynamic corrections in strong-field gravity and their potential astrophysical signatures.

REFERENCES

[1] Ronald A. Remillard and Jeffrey E. McClintock. X-ray properties of black-hole binaries. *Ann. Rev. Astron. Astrophys.*, 44:49–92, 2006.
[2] Erik Verlinde. Emergent gravity and the dark universe. *SciPost Physics*, 2(3):016, 2017.
[3] Valeri P. Frolov. Notes on nonsingular models of black holes. *Phys. Rev. D*, 94(10):104056, 2016.
[4] Sean A. Hayward. Formation and evaporation of non-singular black holes. *Phys. Rev. Lett.*, 96:031103, 2006.
[5] L. Stella and M. Vietri. Lense–thirring precession and quasi-periodic oscillations in low-mass x-ray binaries. *Phys. Rev. Lett.*, 82:17, 1999.
[6] M. Méndez T. Belloni and H. Muñoz-Darias. The distribution of frequencies of twin khz quasi-periodic oscillations in bright low-mass x-ray binaries. *MNRAS*, 426:1701–1709, 2012.
[7] Event Horizon Telescope Collaboration. First m87 event horizon telescope results. i. the shadow of the supermassive black hole. *Astrophys. J. Lett.*, 875(1):L1, 2019.
[8] B. P. Abbott et al. (LIGO Scientific Collaboration and Virgo Collaboration). Observation of gravitational waves from a binary black hole merger. *Phys. Rev. Lett.*, 116:061102, 2016.
[9] Yixin Liu and Yungui Gong. Comparison of verlinde's emergent gravity with mond and dark matter models. *The European Physical Journal C*, 77:691, 2017.
[10] Mariano Cadoni and Enis Belgacem. Galaxy rotation curves from verlinde's emergent gravity and dissipative dark matter. *Phys. Rev. D*, 106:104010, 2022.
[11] Kimet Jusufi. Quasinormal modes of black holes surrounded by dark matter and their connection with the shadow radius. *Phys. Rev. D*, 100(8):084055, 2019.
[12] James Bardeen. Non-singular general-relativistic gravitational collapse. *Proceedings of GR5*, 1968.
[13] Suvankar Chakraborty and Subhendra Mohanty. Quasiperiodic oscillations in black holes: A comparison of general relativity and modified gravity. *Phys. Rev. D*, 104(2):024019, 2021.
[14] R. A. Konoplya and A. Zhidenko. Quasinormal modes of black holes: From astrophysics to string theory. *Rev. Mod. Phys.*, 83:793, 2011.
[15] Cosimo Bambi. Testing the space-time geometry around black hole candidates with the analysis of the broad kα iron line. *Phys. Rev. D*, 85(4):043002, 2012.
[16] Didier Barret. Quasi-periodic oscillations in neutron-star and black-hole x-ray binaries: an overview. *New Astronomy Reviews*, 95:101659, 2022.
[17] Gabriel Török et al. Models of quasi-periodic oscillations as probes of neutron star structure. *Astron. Nachr.*, 332:915, 2011.
[18] Ying Zhang and Songbai Chen. Quasinormal modes and shadows of einstein–born–infeld black holes. *Eur. Phys. J. C*, 79:712, 2019.